

ORIGINAL ARTICLE

Transmembrane channel activity in human hepatocytes and cholangiocytes derived from induced pluripotent stem cells

Rodrigo M. Florentino^{1,2} | Qin Li³ | Michael C. Coard¹ | Nils Haep¹  | Takashi Motomura¹ | Ricardo Diaz-Aragon¹ | Lanuza A. P. Faccioli¹ | Sriram Amirneni¹ | Zehra N. Kocas-Kilicarslan¹ | Alina Ostrowska^{1,2} | James E. Squires^{2,4}  | Andrew P. Feranchak^{2,3} | Alejandro Soto-Gutierrez^{1,2,5}

¹Department of Pathology, University of Pittsburgh School of Medicine, Pittsburgh, Pennsylvania, USA

²Pittsburgh Liver Research Center, University of Pittsburgh, Pittsburgh, Pennsylvania, USA

³Department of Pediatrics, University of Pittsburgh Medical Center, Pittsburgh, Pennsylvania, USA

⁴Division of Gastroenterology, Hepatology, and Nutrition, University of Pittsburgh Medical Center, Pittsburgh, Pennsylvania, USA

⁵McGowan Institute for Regenerative Medicine, Pittsburgh, Pennsylvania, USA

Correspondence

Andrew Feranchak, Department of Pediatrics, Children's Hospital of Pittsburgh of University of Pittsburgh Medical Center, Rangos Research Center, 7th Floor, 4401 Penn Ave., Pittsburgh, PA 15224, USA.

Email: andrew.feranchak@chp.edu

Alejandro Soto-Gutierrez, Department of Pathology, University of Pittsburgh, 200 Lothrop Street, 423 Biomedical Science Tower, Pittsburgh, PA 15261, USA.

Email: als208@pitt.edu

Funding information

National Institutes of Health; Grant/Award Nos. DK078587, DK096990, DK099257, DK117881, DK119973, P30DK120531, and TR002383

Abstract

The initial creation of human-induced pluripotent stem cells (iPSCs) set the foundation for the future of regenerative medicine. Human iPSCs can be differentiated into a variety of cell types in order to study normal and pathological molecular mechanisms. Currently, there are well-defined protocols for the differentiation, characterization, and establishment of functionality in human iPSC-derived hepatocytes (iHep) and iPSC-derived cholangiocytes (iCho). Electrophysiological study on chloride ion efflux channel activity in iHep and iCho cells has not been previously reported. We generated iHep and iCho cells and characterized them based on hepatocyte-specific and cholangiocyte-specific markers. The relevant transmembrane channels were selected: cystic fibrosis transmembrane conductance regulator, leucine rich repeat-containing 8 subunit A, and transmembrane member 16 subunit A. To measure the activity in these channels, we used whole-cell patch-clamp techniques with a standard intracellular and extracellular solution. Our iHep and iCho cells demonstrated definitive activity in the selected transmembrane channels, and this approach may become an important tool for investigating human liver biology of cholestatic diseases.

Rodrigo M. Florentino, Qin Li, Michael C. Coard, Andrew P. Feranchak, and Alejandro Soto-Gutierrez contributed equally to this work.

This is an open access article under the terms of the [Creative Commons Attribution-NonCommercial-NoDerivs](https://creativecommons.org/licenses/by-nc-nd/4.0/) License, which permits use and distribution in any medium, provided the original work is properly cited, the use is non-commercial and no modifications or adaptations are made.

© 2022 The Authors. *Hepatology Communications* published by Wiley Periodicals LLC on behalf of American Association for the Study of Liver Diseases.

INTRODUCTION

Induced pluripotent stem cells (iPSCs) are a form of pluripotent stem cell originating from adult somatic cells.^[1,2] These specialized cells achieve embryonic stem cell–like properties through reprogramming.^[3] In 2007, the Yamanaka lab at Kyoto University was able to generate human iPSCs from human dermal fibroblasts via introduction and subsequent forced expression of distinct transcription factors: Oct3/4, Sox2, Klf4, and c-Myc.^[4] The human iPSCs produced were similar to human embryonic stem cells in morphology, proliferation, gene expression, and epigenetic status of pluripotent cell-specific genes.^[4] An application that has been reliably advantageous is the use of iPSCs to create various cell lines through differentiation.^[2,4–10] In addition, iPSCs derived from somatic cells with disease-related phenotypes can be used to understand the molecular mechanisms of diseases.^[1] Disease modeling with iPSCs is greater to animal models and human cell lines due to the ability of researchers to create patient-specific cells.^[11]

Several reports have created relatively successful protocols for the generation of hepatocyte-like cells (iHep) and cholangiocyte-like cells (iCho) with different levels of maturation.^[5,6,9,10] Based on the results found in a microarray of fetal and adult human hepatocytes, we improved the generation of iHep cells using additional growth factors and molecules, which yielded cells with gene-expression profiles and features that are more comparable to their human adult primary cell counterparts.^[2,12] In recent years, studies have shown successful differentiation to iCho with the cells expressing cholangiocyte markers: cytokeratin 7 and cytokeratin 19 (CK19) as well as cystic fibrosis transmembrane conductance regulator (CFTR) and inositol 1,4,5-trisphosphate receptor type 3 (ITPR3), a protein involved in the cholangiocyte functionality.^[2,6,9] Moreover, researchers have been able to mimic and understand organ development and disease processes by generating specialized cells using the organoid formation approach.^[13,14] Human iPSC-derived liver cells have been also used to create mini human liver as a unit for transplant and as a tool to understand molecular biology in human nonalcoholic steatohepatitis.^[2,10]

Ion chloride (Cl⁻) channels are important to maintain the liver functionality. Movement through the plasma membrane in hepatic cells is performed by specific transmembrane channels such as CFTR, leucine rich repeat-containing 8 subunit A (LRRC8A), and transmembrane member 16 subunit A (TMEM16A).^[15,16] CFTR is expressed exclusively at the apical membrane of cholangiocytes and is activated by intracellular cyclic adenosine monophosphate (cAMP) contributing to the bile formation.^[16,17] TMEM16A, also involved in bile production, is activated by alteration in intracellular

calcium content and has an additional role in the ductular bile formation.^[18–20] The role of TMEM16A in the biliary epithelial cells has been studied; however, the expression of TMEM16A in human hepatocytes has been recently correlated with metabolic disorders.^[21] LRRC8A, a member of the volume-regulated anion channels (VRACs), can be found in both cells (hepatocytes and cholangiocytes).^[15,22] Changes in osmolarity activate LRRC8A, preventing huge alterations in cell size, consequently reducing cell damage.^[23,24] Alteration in the expression and functionality of these channels have been linked to the physiopathology of several cholestatic diseases.^[25,26]

To understand whether human iPSC differentiated hepatocytes and cholangiocytes can be used to study transmembrane channel activity, we sought to establish their functionality through the measurement and analysis of currents in three important transmembrane channels—CFTR, LRRC8A, and TMEM16A, because the activation of these channels is crucial for Cl⁻ efflux across the plasma membrane and contributes to the bile formation process in adult livers.^[17–19,27] Here we characterized the CFTR, LRRC8A, and TMEM16A activity in human iPSC differentiated hepatocytes and cholangiocytes and demonstrated that these cells can be used to model not only hepatocyte and cholangiocyte active transport processes, but also to further understand cholestasis diseases progression, to search for targets and drug screening.

MATERIALS AND METHODS

Cell culture and detailed protocols for differentiation of human iPSCs into hepatocytes (iHep) and cholangiocytes (iCho) are described in the [Supporting Information](#).

Real-time polymerase chain reaction

To characterize the cells, total RNA was isolated from the cells in the end of the iHep or iCho differentiation protocol using Rneasy Mini kits (QIAGEN, Hilden, Germany) and reverse-transcribed using Super-Script III (Invitrogen, Carlsbad, CA, USA) following the manufacturers' instructions. We performed quantitative polymerase chain reaction (PCR) with a StepOnePlus system (Applied Biosystems, Foster City, CA, USA) using TaqMan Fast Advanced Master Mix (Life Technologies, Waltham, MA, USA). The probes used are found in the [Supporting Information](#). Relative gene expression was normalized to β -actin messenger RNA (mRNA). Relative expression was calculated using the $\Delta\Delta$ CT method. Normal primary adult hepatocytes were used as a positive control for the iHep differentiation, and primary hepatocellular carcinoma (PHC) and H69

cells for the iCho protocol. All of the data were normalized to undifferentiated iPSCs.

Immunofluorescence

At the end of the differentiation, iHep and iCho cells were washed once with phosphate buffered saline (PBS), fixed with 4% paraformaldehyde for 15 min, and washed another 3 times with PBS. Samples were washed 3 times with wash buffer (PBS, 0.1% bovine serum albumin [BSA], and 0.1% TWEEN 20) for 5 min and then blocked and permeabilized in blocking buffer (PBS, 10% normal donkey or goat serum, 1% BSA, 0.1% TWEEN 20, and 0.1% Triton X-100) for 1 hour at room temperature. Samples were then incubated with primary antibody in blocking buffer overnight at 4°C. Samples were washed 3 times with wash buffer for 5 min and incubated with secondary antibody in blocking buffer for 1 hour in the dark at room temperature. Then, the samples were washed 3 times with a wash buffer for 5 min, 3 times with PBS, and then counterstained with 1 µg/ml of DAPI (4',6-diamidino-2-phenylindole; Sigma-Aldrich, St. Louis, MO, USA) for 1 min at room temperature in the dark. Samples were washed 3 times with PBS and stored in the dark at 4°C. Samples were imaged using an Eclipse Ti inverted microscope (Nikon) and the NIS-Elements software platform (Nikon). A table with the details relating to the antibodies can be found in the [Supporting Information](#). Normal primary adult hepatocytes were used as a positive control for the iHep differentiation, and primary human cholangiocytes and H69 cells for the iCho protocol.

Western blotting

iHep, iCho, H69, human hepatocyte, and cholangiocyte samples were incubated with radio immunoprecipitation assay lysis buffer (Sigma-Aldrich), 1-times Halt Protease and Phosphatase Inhibitor Cocktail (Thermo Fisher Scientific, Waltham, MA, USA) and incubated for 30 min at 4°C. Samples were centrifuged at 13,000g for 10 min at 4°C. The supernatant from each sample was then transferred to a new microfuge tube and was used as the whole cell lysate. Protein concentrations were determined by comparison with a known concentration of BSA using a Pierce BCA Protein Assay Kit (Thermo Fisher Scientific). A total of 30 µg of lysate was loaded per lane into 10% Mini-PROTEAN TGX gel (Bio-Rad, Hercules, CA, USA). Next, proteins were transferred onto PVDF Transfer Membrane (Thermo Fisher Scientific). Membranes were incubated with primary antibody solution overnight and then washed. Membranes were incubated for 1 hour in secondary antibody solution and then washed. Target antigens were finally detected using SuperSignal West Pico

PLUS Chemiluminescent Substrate (Thermo Fisher Scientific). Images were scanned and analyzed using ImageJ software. All band density values were normalized to the band density for glyceraldehyde 3-phosphate dehydrogenase (GAPDH). The details pertaining to the antibodies can be found in the [Supporting Information](#).

Bile acid

At the end of the hepatocyte differentiation protocol, the medium was replaced to Stage 4 medium without ursodeoxycolic acid. Forty-eight hours later the medium was collected, and a reaction with 3 alpha-hydroxysteroid dehydrogenase was measured by fluorescence intensity using the Bile Acid Assay Kit (Sigma-Aldrich), according to the manufacturer's instructions.

cAMP levels

iCho and PHC were plated in a collagen-coated 96-well plate the day after the cells were stimulated with 10 µM secretin or 10 µM Forskolin (Cayman Chemical, Ann Arbor, MI, USA). cAMP levels were measured using the cAMP-Glo assay kit (Promega, Madison, WI, USA) according to the manufacturer's instructions.

Cholyl-lysyl-fluorescein transport assay

The experiment was performed as previously described by Sampaziotis et al. with some modifications.^[6] At the end of Stage 4 for the cholangiocyte differentiation protocol, the cells were detached and 2×10^4 cells were replated in a thick layer of Matrigel Basement Membrane Matrix (Corning, New York, NY, USA). Cells were then further differentiated into mature cholangiocytes using maturation medium (Stage 5). Ten days later the cells were incubated with 5 µM of cholyl-lysyl-fluorescein (CLF; Corning) or 5 µM of unconjugated fluorescein isothiocyanate (Sigma-Aldrich) as control. After 30 min at 37°C, cells were washed with Leibovitz's medium (Life Technologies, Waltham, MA, USA), and images were taken right after (loading phase) and 10 min later (exporting phase). Samples were imaged using an Eclipse Ti inverted microscope (Nikon), and the NIS-Elements software platform (Nikon) and measurements were made using Image J software.

Measurement of Cl⁻ currents

Membrane currents were measured via whole-cell patch clamp techniques. Cells on a cover slip were mounted in a chamber (volume ~400 µl), and whole-cell currents

were measured using specific intracellular and extracellular solutions as described subsequently. Patch pipettes were pulled from Corning 7052 glass and had a resistance of 2–5 M Ω . Recordings were made with an Axopatch ID amplifier (Axon Instruments, Foster City, CA, USA) and were filtered at 2 kHz and sampled at 4 kHz for storage on a computer and analyzed using pCLAMP version 10 (Axon Instruments, Burlingame, CA, USA) as previously described.^[18,19] Two voltage protocols were used: (1) holding potential –40 mV, with rapid alteration of membrane potential from –100 mV to +100 mV over 450 ms every 2 seconds (RAMP protocol), and (2) holding potential –40 mV, with 450-ms steps from –100 mV to +100 mV in 20-mV increments (STEP protocol). Protocol 1 was used for real-time tracings, and Protocol 2 for generation of current-voltage (I-V) plots. Results are compared with control studies measured on the same day to minimize any effects of day-to-day variability and reported as current density (pA/pF) to normalize for differences in cell size. Solutions used to maximize potential cAMP-stimulated Cl⁻ currents (e.g., CFTR) included a pipette solution containing 150 mM *N*-methyl-D-glucamine-Cl, 1 mM MgCl₂, 1 mM ethylene glycol tetraacetic acid (EGTA), 0.5 mM adenosine triphosphate (ATP), and 10 mM 4-(2-hydroxyethyl)-1-piperazine ethanesulfonic acid (HEPES) at pH 7.3; and a bath solution containing 150 mM *N*-methyl-D-glucamine-Cl, 1 mM MgCl₂, 1 mM CaCl₂, and 10 mM HEPES-Tris at pH 7.4. Solutions used to maximize potential volume-stimulated Cl⁻ currents (e.g., LRRC8A) included a pipette solution containing 90 Cs-chloride, 50 Cs-aspartate, 1 mg ATP, 10 mM HEPES, and 2 mM EGTA at pH 7.3, buffered with CsOH; and a bath solution containing 85 mM NaCl, 1 mM CaCl₂, 1 mM MgCl₂, 10 mM HEPES, 120 mM D-mannitol, and 10 mM glucose at pH 7.4, buffered with NaOH. Osmolarity was adjusted with D-mannitol to 310 \pm 5 mOsm/kg (isotonic) using an Advanced Micro Osmometer (Model 3300; Advanced Instruments Inc., Norwood, MA, USA). Cell swelling was induced by omitting a defined concentration of mannitol from the bath solution to induce hypotonicity (up to 190 mOsm/kg). Solutions used to maximize potential Ca²⁺-activated Cl⁻ currents (e.g., TMEM16A) included the pipette solution containing 130 mM KCl, 10 mM NaCl, 2 mM MgCl₂, 10 mM HEPES/KOH, 0.5 mM CaCl₂, 3 mM MgATP²⁻, and 1 mM EGTA (pH 7.3); and a bath solution containing 140 mM NaCl, 4 mM KCl, 1 mM CaCl₂, 2 mM MgCl₂, 1 mM KH₂PO₄, 10 mM glucose, and 10 mM HEPES/NaOH (pH \sim 7.4). A total of 10 μ M CFTRinh-172 (Millipore, Billerica, MA, USA) and 10 μ M T16Ainh-A01 (Millipore, Billerica, MA, USA) were used to inhibit CFTR and TMEM16A current, respectively.

Statistical analysis

For statistical analysis, means between two groups were compared by *t* test. Comparison of multiple

groups was performed by one-way analysis of variance followed by the Tukey *post hoc* test, according to the number of independent groups, unless otherwise stated. Data are reported as means \pm SD. A *p* value < 0.05 was considered as statistically significant.

RESULTS

Differentiation of human iPSCs into iHep

To induce differentiation of the human iPSCs into iHep, we used our previously published protocol.^[2,10] The endoderm induction steps were cultured using a monolayer system (Figure 1A). As a result, more than 85% of the cells expressed the definitive endoderm marker, SRY-BOX 17 (Sox17) (Figure 1B) at Day 4. For hepatic specification, cells were treated with dimethyl sulfoxide (DMSO) and hepatocyte growth factor (HGF) for 10 days. The last 4 days the cells were replated and cultured with growth factors to induce maturation.^[2] mRNA analyses were performed on the iHep cells to observe the relative expression of mature hepatocyte-specific markers (hepatocyte nuclear factor 4 α [HNF4 α], liver X receptor [LXR], and UDP glucuronosyltransferase family 1 member A1 [UGT1A1]) (Figure 1C), as well as the loss of the pluripotent markers Nanog and OCT3/4 (Figure S3). It is important to note that HNF4 α and LXR are liver-enriched transcription factors, which are vital in organ development and cellular function.^[28] The analyses revealed the up-regulation of HNF4 α and LXR in iHep to levels comparable to the human adult primary hepatocyte (Figure 1C), with more than 85% of cell nuclei expressing HNF4 α at the protein level (Figure 1D). Liver-enriched transcription factors such as HNF4 α and LXR act as regulators for relevant genes, including UGT1A1.^[29] Up-regulation of HNF4 α and LXR in iHep subsequently induced the expression of UGT1A1, although at levels significantly lower than in human adult hepatocytes, as already described.^[2] The relative expression of cholangiocyte-specific markers (Sox9, HNF1 β , and ITPR3) was measured in iHep, to further establish absolute characterization of our cells (Figure 1C). Despite progress in advancing the differentiation of human stem cells into hepatocytes *in vitro*, cells that replicate the ability of human primary adult hepatocytes to metabolize drugs *in vitro* and other mature advanced functions, we have developed a chemically defined system to generate functional hepatocytes with some characteristics of a mature phenotype.^[2] As a result, up-regulation of the cholangiocyte markers at the mRNA level was observed within our iHep cells. However, at the completion of the differentiation protocol, nearly 100% of the cells expressed albumin, adult isoform of HNF4 α , but did not express alpha-fetoprotein (AFP), an immature

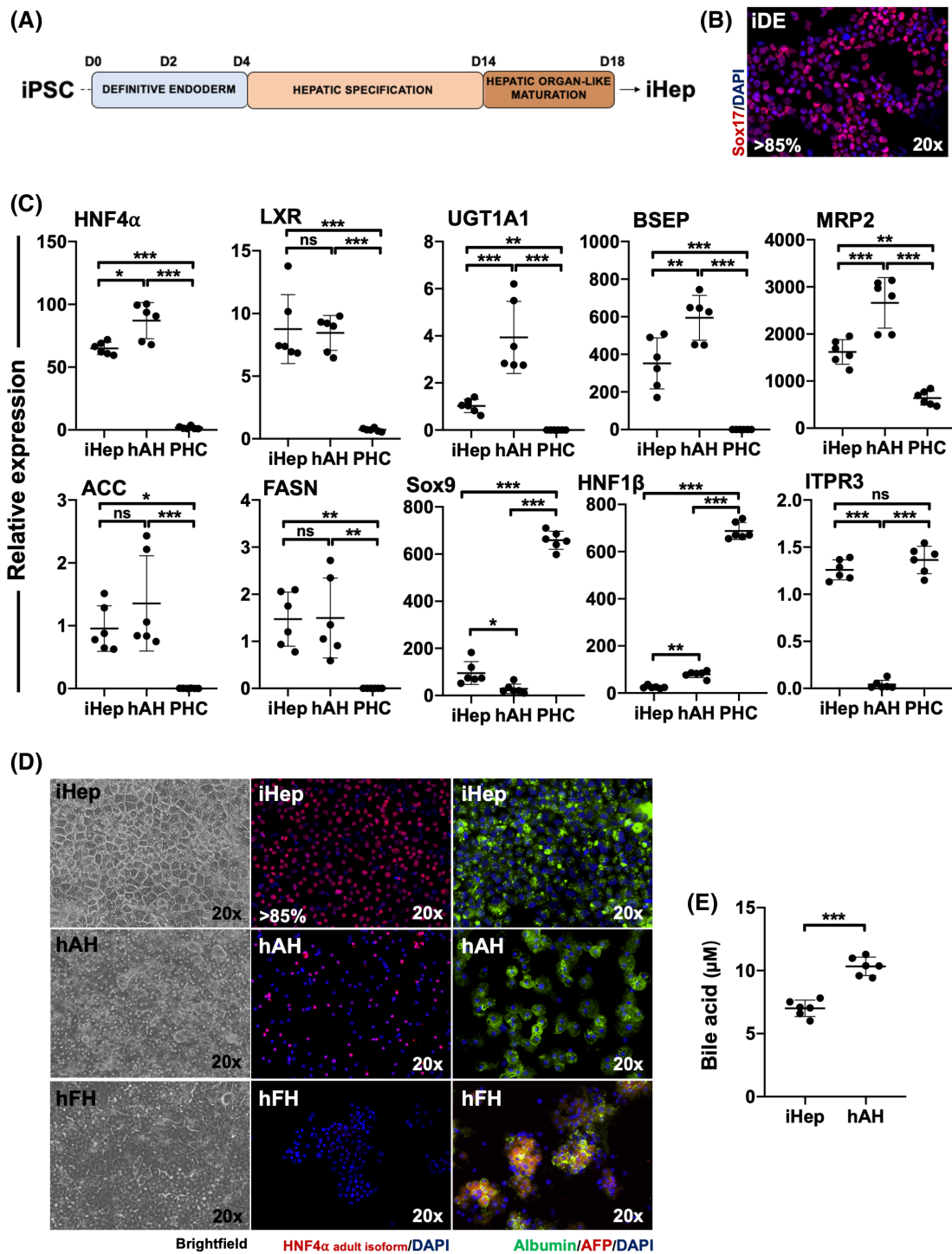


FIGURE 1 Generation and characterization of hepatocytes from human-induced pluripotent stem cells (iPSCs). (A) Schematic depiction of the protocol used to differentiate human iPSCs to human-induced iPSCs (iHep). (B) Immunofluorescence analysis exhibiting expression of a crucial endoderm marker using an antibody that recognized SRY-box 17 (Sox17) at day 4. (C) Messenger RNA (mRNA) analyses of the expression of hepatocyte-specific genes: adult isoform of hepatocyte nuclear factor 4 α (HNF4 α), liver X receptor (LXR), UDP glucuronosyltransferase family 1 member A1 (UGT1A1), bile salt export pump (BSEP), multidrug resistance-associated protein 2 (MRP2), acetyl-CoA carboxylase alpha (ACC), and fatty acid synthase (FASN); and cholangiocyte-specific genes: Sox9, HNF1 β , and inositol 1,4,5-triphosphate receptor, type 3 (ITPR3). Values are determined relative to β -actin and presented as fold change relative to the expression in human iPSCs at day 0, which is set as 1. Error bars represent mean \pm SD of three independent experiments (* p < 0.05; ** p < 0.01 and *** p < 0.001). (D) Immunofluorescence analyses exhibiting expression of key hepatocyte markers at day 18, while using antibodies that recognized the adult isoform of HNF4 α , albumin, and alpha-fetoprotein (AFP). Human adult hepatocytes (hAH) and human fetal hepatocytes (hFH) were used as controls. (E) Comparison of bile acid production between iHep and human adult hepatocytes. Values per million cells. Error bars represent mean \pm SD of three independent experiments (*** p < 0.001). PHC, primary hepatocellular carcinoma

hepatocyte marker (Figure 1D). Moreover, although some mRNA expression of Sox9 (cholangiocyte marker) was detected in iHep at the end of the differentiation protocol, Sox9 protein expression was not detected, indicating their hepatic phenotype (Figure S4).

Hepatocytes are responsible for production of several plasma proteins, detoxification of endogenous and xenobiotics compounds, and are involved in the bile production.^[30] As an active metabolic cells, hepatocytes have a large content of mitochondria, as this organelle is involved in the intracellular energy production through glucose metabolism.^[31] In previous work, we documented that iHep mitochondrial content was similar to that observed in human primary adult hepatocytes.^[2] We also analyzed the ability of iHep to store glycogen and secrete urea and alpha-1-antitrypsin.^[2] Here, we analyzed gene expression of acetyl-CoA carboxylase alpha and fatty acid synthase, genes involved in the lipogenesis process.^[32] As expected, the cells generated by our hepatocyte-directed differentiation protocol showed an up-regulation of both genes, as seen in human hepatocytes (Figure 1C). We also investigated the ability of iHep to secrete bile acids. Moreover, quantitative PCR analyses revealed that bile salt export pump and multidrug resistance-associated protein 2 are expressed in the iHeps (Figure 1C). Finally, iHeps are able to secrete bile acids to the medium comparable to human hepatocytes (Figure 1E).

Differentiation of human iPSCs into iCho cells

To induce differentiation of the human iPSCs into iCho cells, we used our previously published protocol.^[2] Cholangiocytes and hepatocytes share common precursors,^[8] so the endoderm induction steps were identical to the steps used in the hepatocyte differentiation protocol (Figure 2A). At the end of definitive endoderm induction, more than 85% of the cells expressed the endoderm marker Sox17 (Figure 2B). To induce hepatic specification, the endoderm cells were exposed to bone morphogenetic protein 4 (BMP4) and fibroblast growth factor 2 (FGF2) for 5 days. To stimulate cholangiocyte induction, the cells were cultured in activin A, FGF10, and retinoic acid for 4 days. Finally, to ensure the maturation of the iCho cells, we treated the cells with epidermal growth factor (EGF), dexamethasone, interleukin 6, sodium pyruvate, TGF β 1, and sDLL-1 (ligand for Notch receptors) to the differentiation program for 10 days.^[2] Following this treatment, the cells lost the expression of Nanog and OCT3/4 (pluripotent markers) (Figure S3). Additional gene-expression analyses were performed to document the relative expression of mature cholangiocyte-specific markers (Sox9, HNF1 β ,

and ITPR3), an intracellular calcium release channel involved in bicarbonate secretion in bile ducts.^[33] Next, to fully characterize cholangiocyte phenotype of the resulting cells, we evaluated gene expression of functional components within the bile production machinery expressed in the human cholangiocytes. Secretin receptor, Cl⁻/HCO₃⁻ anion exchanger 2, aquaporin 1, cholinergic receptor muscarinic 3, and P2Y purinoceptor 1 were expressed in iCho cells at comparable levels to those in human primary cholangiocyte, controls (Figure 2C). Hepatocyte-specific markers HNF4 α , LXR, and UGT1A1 were no longer expressed or became significantly reduced, showing that our protocol was efficient in generating cholangiocyte-like cells (Figure 2C). Following this last stage, the cells expressed CK7, CK19 and Sox9, markers found in mature bile ducts^[10] (Figure 2D). Next, to assess the functionality of iCho, we measured the intracellular levels of cAMP mediated by secretin and forskolin stimuli (activators of CFTR and consequently involved in the secretion of bicarbonate into the bile duct lumen).^[34] As human primary cholangiocytes, iCho cells were able to elevate the intracellular levels of cAMP following the secretin and forskolin stimuli (Figure 2E). iCho were also able to export bile acids, measured by the exportation of the fluorescent bile acid CLF in a 3D culture (Figure 2F). Recent studies have reported that changes in the bile flow, composition, and osmolarity are detected by proteins expressed through the cilium, thus activating intracellular pathways that are important for bile formation.^[35] Immune staining analysis shows the expression of acetyl- α -tubulin localized on cilia of iCho and human primary cholangiocytes, controls (Figure 2G).

Functional assessment of CFTR

After generating and characterizing iHep and iCho, we analyzed CFTR to establish the functionality of our cells. A mRNA analysis revealed a significant up-regulation of CFTR in iCho cells when compared with the H69 human cholangiocyte cell line. The relative expression of CFTR in iHep was essentially nonexistent, which was comparable to the levels observed in adult human primary hepatocytes (Figure 3A). To further substantiate these findings, a protein analysis showed a strong signal for CFTR in iCho cells, while very weak signals were present in cholangiocyte cell line, H69, and iHep. Quantification of protein expression when normalized with GAPDH indicated a significantly large difference between the presence of CFTR in iCho and H69. Additionally, a slightly significant difference between the CFTR levels in iHeps and adult primary hepatocytes was recorded (Figure 3B). To determine the functional significance of CFTR expression, patch clamp studies were performed in iCho and iHeps. Under basal conditions, little current is observed (-2.1

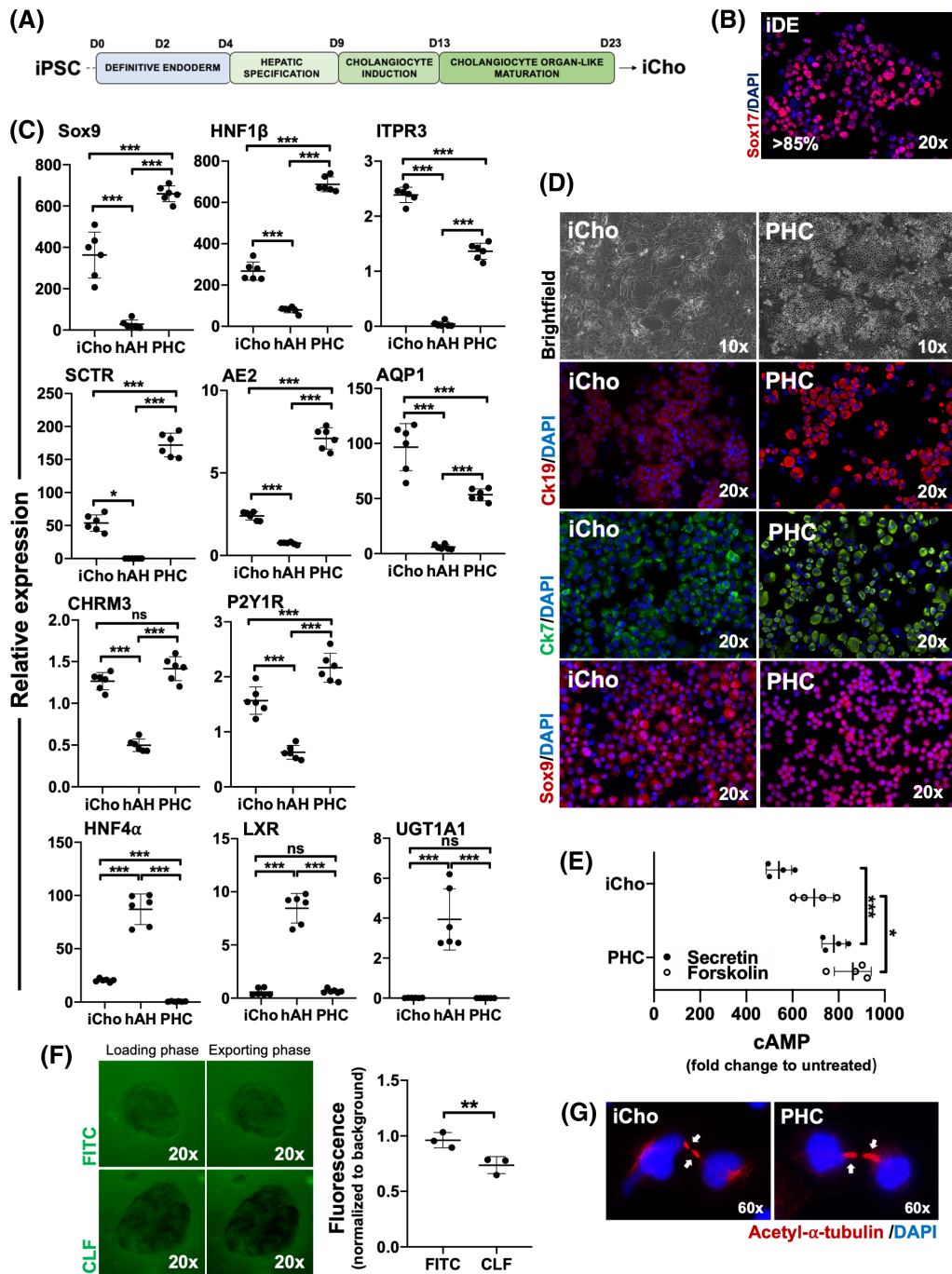


FIGURE 2 Generation and characterization of iPSC-derived cholangiocyte (iCho) cells from human iPSC. (A) Schematic depiction of the protocol used to differentiate human iPSCs to iCho cells. (B) Immunofluorescence analysis exhibiting expression of a crucial endoderm marker using an antibody that recognized Sox17 at day 4. (C) mRNA analyses of the expression of cholangiocyte-specific genes: Sox9, HNF1 β , ITPR3, secretin receptor (SCTR), Cl⁻/HCO₃⁻ anion exchanger 2 (AE2), aquaporin 1 (AQP1), cholinergic receptor muscarinic 3 (CHRM3), P2Y purinoceptor 1 (P2Y1R), and hepatocyte-specific genes: adult isoform of HNF4 α , LXR, and UGT1A1. Values are determined relative to β -actin and presented as fold change relative to the expression in human iPSCs at day 0, which is set as 1. Error bars represent mean \pm SD of three independent experiments (* $p < 0.05$; ** $p < 0.01$, and *** $p < 0.001$). (D) Immunofluorescence analyses exhibiting expression of key cholangiocyte markers at day 23, while using antibodies that recognized cytokeratin 7 (CK7), CK19, and Sox9. Primary human cholangiocyte was used as a control. (E) Measurement of intracellular cyclic adenosine monophosphate (cAMP) in response to secretin (10 μ M) and forskolin (10 μ M) stimuli. Error bars represent mean \pm SD of three independent experiments (* $p < 0.05$ and *** $p < 0.001$). (F) Representative images demonstrating active export of the fluorescent bile acid cholyl-lysyl-fluorescein (CLF) from the lumen of human iCho organoids compared with controls loaded with fluorescein isothiocyanate (FITC). Results show the fluorescence intensity in the center of organoids was normalized to background; error bars represent mean \pm SD of three independent experiments (** $p < 0.01$). (G) Acetyl- α -tubulin staining revealed that the iCho cells have a primary cilium as the primary human cholangiocyte. DAPI, 4',6-diamidino-2-phenylindole

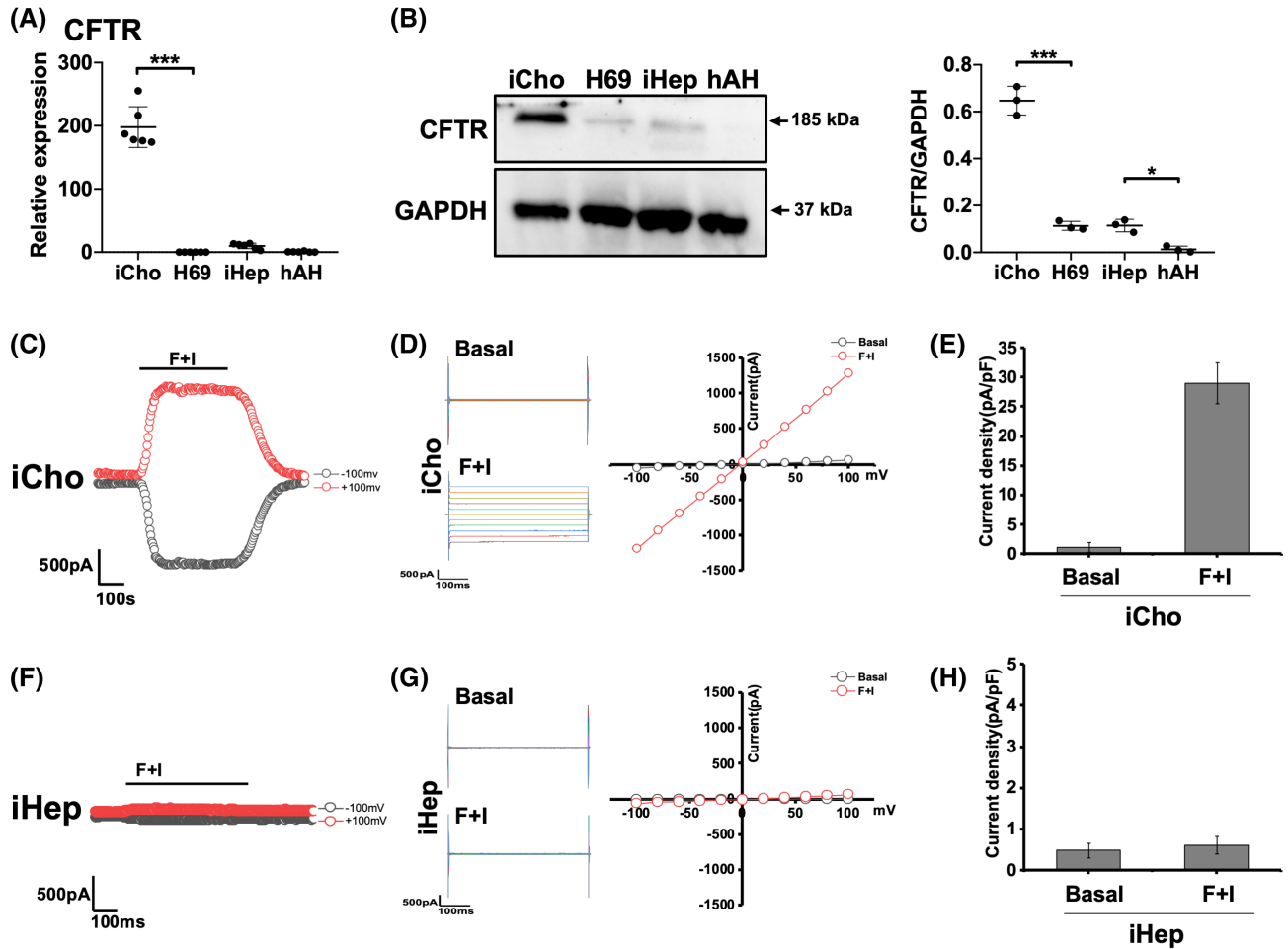


FIGURE 3 Cystic fibrosis transmembrane conductance regulator (CFTR) characterization in human iHep and iCho. (A) mRNA analysis of the expression of CFTR in iCho and iHep. Values are determined relative to β -actin and presented as fold change relative to the expression in human iPSCs at day 0, which is set as 1. Error bars represent mean \pm SD of three independent experiments (** $p < 0.001$). (B) Representative image of the western blot analysis and quantification of CFTR in iCho ($n = 3$) at day 23 and iHep ($n = 3$) at day 14. For normalization, glyceraldehyde 3-phosphate dehydrogenase (GAPDH) was used. H69 cell ($n = 3$) and primary adult human hepatocytes ($n = 3$) were used as controls ($*p < 0.05$ and $***p < 0.001$). (C) Representative whole cell currents of iCho measured during basal conditions and in response to forskolin (10 μ M) and IBMX (100 μ M). Currents measured at -100 mV (black circles) and at $+100$ mV (red circles) are shown. (D) Currents were measured in iCho during basal (control) conditions and in response to forskolin and IBMX using STEP protocol. (E) Current-voltage (I-V) plot generated by STEP protocol. (F) Representative whole cell currents of iHep measured during basal conditions and in response to forskolin (10 μ M) and IBMX (100 μ M). Currents measured at -100 mV (black circles) and at $+100$ mV (red circles) are shown. (G) Currents were measured in iHeps during basal (control) conditions and in response to forskolin and IBMX using STEP protocol. (H) I-V plot generated by STEP protocol

± 0.5 pA/pF at -100 mV); however, in response to a CFTR-activating cocktail that included forskolin (10 μ M) and IBMX (100 μ M), large currents are observed in iCho (-28.5 ± 2.2 pA/pF at -100 mV) (Figure 3C). Currents were linear with a reversal at 0 mV, consistent with the observed biophysical properties of CFTR (Figure 3D,E) and inhibited when the cells were exposed to CFTRinh-172 (Figure S5). In contrast, no currents were observed in iHeps in response to forskolin and IBMX (Figure 3F,G). Current density analysis confirmed that the iCho cells have a great CFTR current when stimulated with the CFTR-activating cocktail, and as expected no current was detected in the iHep cells (Figure 3E,H). These findings are consistent with the functional expression of CFTR in iCho.

Functional assessment of LRRC8A

While only cholangiocytes express CFTR, and not hepatocytes, all cells of the liver exhibit volume-regulated anion currents. In human, rat, and mouse models, both hepatocytes and cholangiocytes demonstrate robust Cl^- currents in response to cell swelling.^[15,22] Recently, in other cell types, LRRC8A was identified as a critical member of the volume-regulated anion channel.^[23,24] To determine whether LRRC8A was present and functional in our cells, functional studies were performed. First, LRRC8A was observed in all models including iHep, iCho, H69, and human adult hepatocytes (hAH) by quantitative PCR. A slightly significant difference between

the expression in iCho and H69 was found, but the difference between expression in iHep and hAH was not found to be significant (Figure 4A). Additionally, a western blot analysis showed a positive result for all of the samples. However, only iCho, iHep, and hAH displayed strong protein expression of LRRC8A; the expression of the cholangiocyte control, H69, was quite weak. Quantification of protein expression when normalized with GAPDH indicated a moderately significant difference between expression in iCho and H69, while the difference between iHep and hAH was not significant (Figure 4B). Next, patch clamp studies were performed to determine whether iCho and iHeps exhibit functional volume-regulated anion channels in response to cell swelling. In iCho, little current activity

was observed under basal (isotonic) conditions ($+4.5 \pm 0.5$ pA/pF at +100 mV); however, in response to hypotonic exposure (190 mOsm), the magnitude of currents increased dramatically (to $+56.8 \pm 3.8$ pA/pF at +100 mV) (Figure 4C). Currents demonstrated time-dependent inactivation at positive membrane potentials, reversal at 0 mV (I_{revCl^-}), and mild outward rectification biophysical properties consistent with LRRC8A^[23] (Figure 4D). Similarly, volume-regulated anion currents were also measured in iHeps with a maximum current density of 17.2 ± 2.6 pA/pF at +100 mV in response to hypotonic exposure, 190 mOsm (Figure 4F,G). Current density analysis confirmed that both of our cells, iCho and iHep, respond to the hypotonic stimuli. However, the response in the

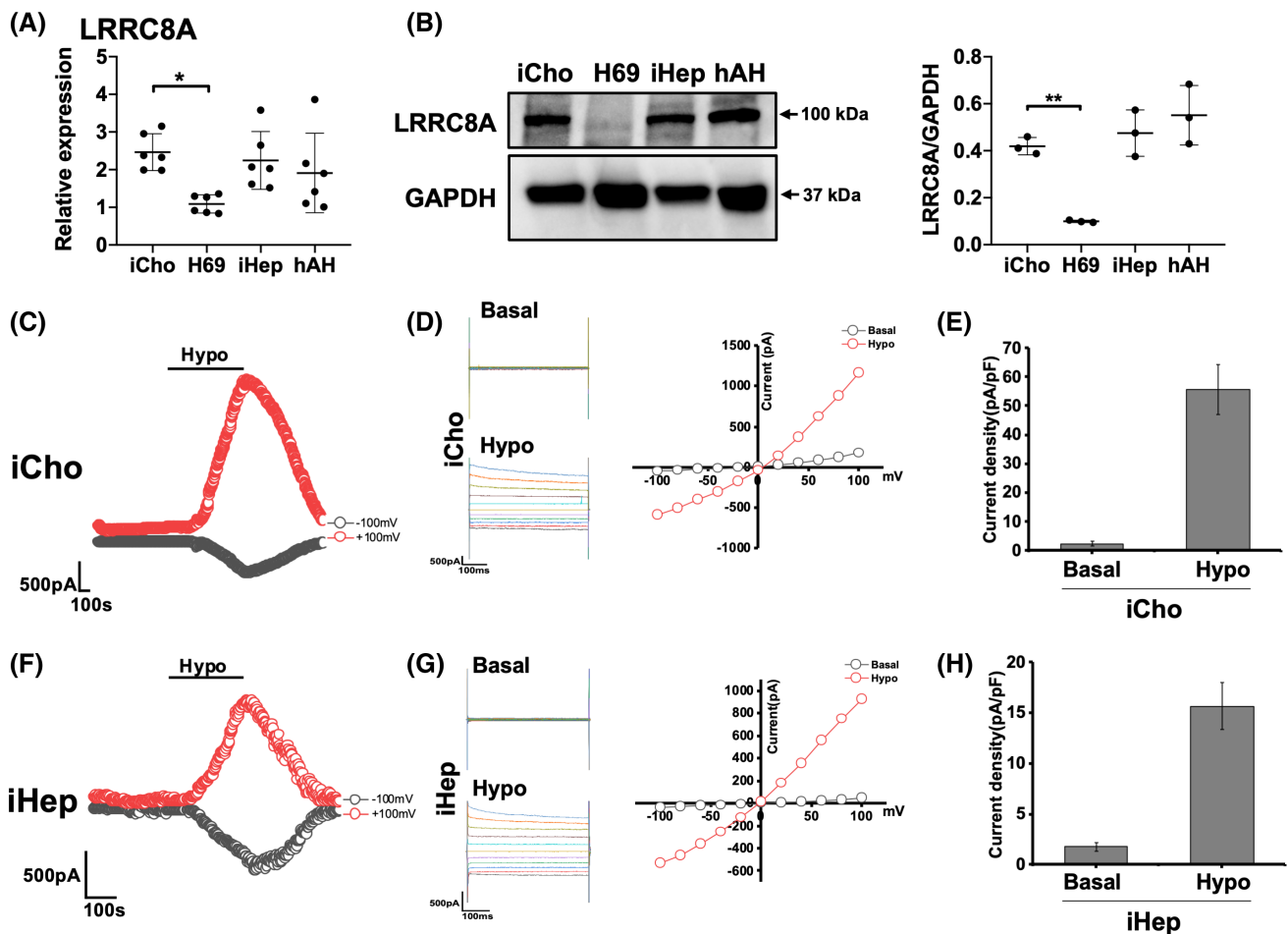


FIGURE 4 Leucine rich repeat-containing 8 subunit A (LRRC8A) characterization in human iHep and iCho. (A) mRNA analysis of the expression of LRRC8A in iCho and iHep. Values are determined relative to β -actin and presented as fold change relative to the expression in human iPSCs at day 0, which is set as 1. Error bars represent mean \pm SD of three independent experiments ($*p < 0.05$). (B) Representative image of the western blot analysis and quantification of LRRC8A in iCho ($n = 3$) at day 23 and iHep ($n = 3$) at day 14. For normalization, GAPDH was used. H69 cell ($n = 3$) and primary adult human hepatocytes ($n = 3$) were used as controls ($**p < 0.01$). (C) Representative whole cell currents in iCho in response to hypotonicity (190 mOsm). Currents measured at -100 mV (black circles) and at $+100$ mV (red circles) are shown. (D) Currents were measured in iCho during basal (control) conditions and in response to hypotonic exposure (Hypo) using STEP protocol. (E) I-V plot generated by STEP protocol showing control (black circles) and hypotonic-stimulated (red circles) currents. (F) Representative whole cell currents of iHeps measured during basal conditions and in response to hypotonicity. Currents measured at -100 mV (black circles) and at $+100$ mV (red circles) are shown. (G) Currents were measured in iHeps during basal (control) conditions and in response to hypotonicity using STEP protocol. (H) I-V plot generated by STEP protocol showing control (black circles) and hypotonic-stimulated (red circles) currents

biliary cell was higher than the induced hepatocyte (Figure 4E,H). Together these findings demonstrate that both iCho and iHep express LRRC8A and exhibit volume-regulated anion currents in response to hypotonicity consistent with LRRC8A.

Functional assessment of TMEM16A

Finally, we investigated functionality through TMEM16A. A mRNA analysis revealed slight up-regulation of TMEM16A in iHep and iCho cells, with very strong expression of TMEM16A within the human adult primary hepatocyte control, hAH. The difference in relative expression between iHep and hAH was slightly significant (Figure 5A). A western blot analysis showed a definitively positive result for iCho, iHep, and hAH. Quantification of protein expression when normalized with GAPDH confirmed the presence and protein expression of TMEM16A within all of the samples. A moderately significant difference was observed between expression in iHep and hAH, while the difference between iCho and H69 was not significant (Figure 5B). Previously, we have shown that cholangiocytes exhibit large TMEM16A-mediated Cl^- currents in response to extracellular ATP, which increases intracellular Ca^{2+} concentration.^[20,36] Under patch clamp conditions, iCho exhibited only small currents during basal conditions; however, in response to ATP (100 μM), the magnitude of currents increased significantly to 12.4 ± 2.5 pA/pF at +100 mV. Currents displayed time-dependent activation, outward rectification, and reversal at 0 mV when ATP was removed (no-ATP phase), properties consistent with TMEM16A.^[36] An inhibition of the TMEM16A current was recorded when the iCho was exposed to T16Ainh-A01 (Figure S6). In contrast, iHeps exhibited only very small ATP-mediated Cl^- currents in comparison with iCho, even though an inhibition of the current can be observed when T16Ainh-A01 (TMEM16A inhibitor) is used (Figure S7). Together, these studies demonstrate that both iCho and iHep express TMEM16A channels, although the magnitude of current density is significantly larger in iCho compared with iHep.

DISCUSSION

iPSCs have been used broadly as a model to understand biological processes and the physiopathology of several diseases.^[37] The forced expression of specific transcription factors in somatic cells allows these cells to resemble embryonic stem cells in the expression of pluripotency markers and differentiation into three germ layers (endoderm, mesoderm, and ectoderm).^[4] Consequently, researchers have been able to model different organs such as the liver, heart, and brain.^[2,38,39] In our current study, we differentiated iPSCs into two

important cell types within the liver, hepatocytes and cholangiocytes, using our well-established differentiation protocol.^[2,10] Furthermore, we characterized both cell types by the level of activity in transmembrane channels: CFTR, LRRC8A, and TMEM16A. We successfully produced differentiated hepatocytes and cholangiocytes, which possessed components for the activity of chloride ion mobilization through the plasma membrane.

Several protocols have been reported to generate hepatocytes: the major cell type of the liver parenchyma.^[2,10,40,41] Using different growth factors and small molecules, most protocols are able to generate induced hepatocytes with fetal features, indicated by the expression of AFP and in some cases epithelial cell adhesion molecule, a hepatoblasts marker.^[5,42] Collin de l'Hortet et al. modified previous protocols to differentiate iPSCs into hepatocytes with more mature characteristics. In a monolayer, instead of a 3D culture, the definitive endoderm was induced using a combination of bFGF2, hBMP4, and activin A. For hepatocyte specification, HGF and DMSO were used.^[10] Recently, a fourth stage was added to Collin de l'Hortet et al.'s protocol to reach a higher level of maturation. Based on the results found in a microarray of fetal and adult human hepatocytes, the cells were cultured in low glucose with addition of free fatty acids (palmitic and oleic acid), bile acids (ursodeoxycholic acid), cholesterol, corticoids (dexamethasone and hydrocortisone), EGF, and rifampicin to increase maturation. More than 70% of the cells generated by this protocol had nuclear expression of the adult isoform of HNF4 α ; all of the cells expressed albumin and did not express AFP.^[2] These results were reproduced in this current study (Figure 1).

On the contrary, few protocols have been reported to induce cholangiocyte-like cells.^[6,9,43] Cholangiocytes share the same germ layer as hepatocytes; therefore, the definitive endoderm was induced using the same initial steps as the hepatocyte protocol.^[2,8] Cholangiocyte specification and maturation was done by treating the cells with several growth factors and molecules, TGF β 1 and sDLL-1. These growth factors and molecules are responsible for the activation of the Notch and TGF β signaling pathways, which are involved in the biliary commitment of hepatoblasts.^[7,44–46] mRNA and protein analysis, as functional assays, demonstrated that the induced cholangiocytes generated by our protocol were relatively close to primary human cells.^[2] Using the same protocol, our iCho cells expressed biliary markers at the mRNA level, in addition to CK7, CK19, and Sox9 at the protein level compared with primary cholangiocytes (Figure 2).

To investigate whether our protocol to differentiate human iPSCs into hepatocytes and cholangiocytes was able to generate a functional hepatic cell, we analyzed the activity of transmembrane channels involved in liver functions. Bile formation, one of the major liver functions, is a combination of hepatocyte

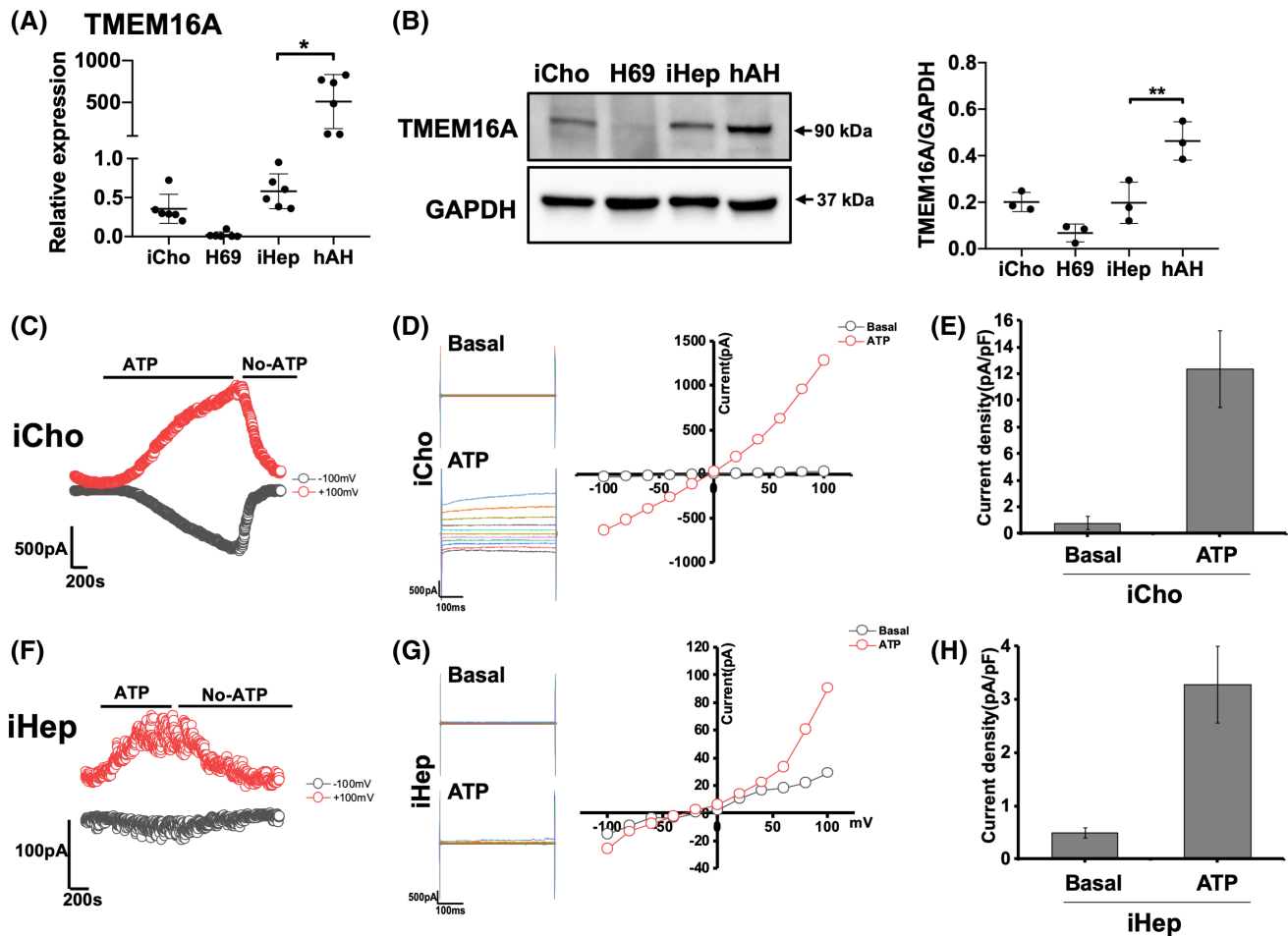


FIGURE 5 Transmembrane member 16 subunit A (TMEM16A) characterization in human iHep and iCho. (A) mRNA analysis of the expression of TMEM16A in iCho and iHep. Values are determined relative to β -actin and presented as fold change relative to the expression in human iPSCs at day 0, which is set as 1. Error bars represent mean \pm SD of three independent experiments ($*p < 0.05$). (B) Representative image of the western blot analysis and quantification of TMEM16A in iCho ($n = 3$) at day 23 and iHep ($n = 3$) at day 14. For normalization, GAPDH was used. H69 cell ($n = 3$) and primary adult human hepatocytes ($n = 3$) were used as controls ($**p < 0.01$). (C) Representative whole cell currents in iCho in response to extracellular adenosine triphosphate (ATP) (100 μ M). Currents measured at -100 mV (black circles) and at $+100$ mV (red circles) are shown. (D) Currents were measured in iCho during basal (control) conditions and in response to ATP using STEP protocol. (E) I-V plot generated by STEP protocol showing control (black circles) and ATP-stimulated (red circles) currents. (F) Representative whole cell currents of iHeps measured during basal conditions and in response to ATP. Currents measured at -100 mV (black circles) and at $+100$ mV (red circles) are shown. (G) Currents were measured in iHeps during basal (control) conditions and in response to ATP using STEP protocol. (H) I-V plot generated by STEP protocol showing control (black circles) and ATP-stimulated (red circles) currents

and cholangiocyte processes.^[47] Hepatocytes are responsible for the uptake and/or production and metabolism of bile salts, which are secreted in the biliary canaliculus.^[47] Through complex mechanisms and different modes of activation, transmembrane channels in the apical membrane of the cholangiocytes move chloride ions to enhance the secretion of bicarbonate into the lumen of the bile duct.^[47] CFTR, expressed at the apical membrane of biliary cells, is one of the transmembrane channels.^[17,48] Our iCho cells showed great activation of CFTR in the presence of the stimuli. However, as expected, there was no difference observed in the iHep, because this channel is only expressed in cholangiocytes. Calcium-mediated activation of TMEM16A with ATP stimuli was also

measured in our iCho cells. According to the results, the cholangiocyte-like cells produced by our protocol mimic the functions and features of the bile process formation. The expression of TMEM16A in human hepatocytes is not well reported. Recent publications have shown the correlation between TMEM16A and metabolic disorders in the liver.^[21] In our system, mRNA and protein analysis revealed the expression of TMEM16A in our iHep and in the human adult hepatocytes (Figure 5A,B). However, slight activity was observed, but was not comparable with the activity recorded in the iCho. More studies need to be performed to truly understand the role of TMEM16A in human hepatocytes. Finally, we analyzed LRRC8A, a member of the VRACs. Osmoregulation is important in

all cell types to maintain functionality at metabolic and biochemical levels, although it is critical for the cells of the liver, which are potentially exposed to changes in osmolarity between fed and fasted states.^[49] Importantly, both iHep and iCho cells exhibited robust volume-activated Cl⁻ currents when exposed to hypotonic conditions. The role of volume-regulated Cl⁻ channels in coupling cellular metabolism to cell size, as well as maintaining membrane integrity, deserves further study in both iHeps and iCho.

In summary, our results showed that both of our protocols are able to successfully generate differentiated induced hepatocytes and cholangiocytes. The cells produced in this study not only express their markers at mRNA and protein levels, but also showed functionality at these transmembrane channels. The generation of more reliable models to study liver diseases and a platform for drug screening are available with the reprogramming of somatic cells from patients with genetic diseases and the production of human-induced hepatocytes and cholangiocytes.

ACKNOWLEDGMENT

This work was supported by NIH grant 1P30DK 120531-01 to Pittsburgh Liver Research Center (PLRC) and the PLRC sponsored Director's Award in New Direction and Innovation to R.M.F. The authors thank Carla Frau for the administrative support.

CONFLICT OF INTEREST

A.S-G. has a provisional international patent application that describes hepatic differentiation of human pluripotent stem cells and liver repopulation (PCT/US2018/018032). A.S-G., is a co-founder and has a financial interest in Von Baer Wolff, Inc., a company focused on biofabrication of autologous human hepatocytes from stem cells technology. A.S-G., and A.O. are cofounders and have a financial interest in Pittsburgh ReLiver Inc., a company focused on programming liver failure and their interests are managed by the Conflict-of-Interest Office at the University of Pittsburgh in accordance with their policies.

ORCID

Nils Haep  <https://orcid.org/0000-0001-8149-4011>

James E. Squires  <https://orcid.org/0000-0001-6979-8987>

REFERENCES

- Ye L, Swingen C, Zhang J. Induced pluripotent stem cells and their potential for basic and clinical sciences. *Curr Cardiol Rev*. 2013;9:63–72.
- Takeishi K, Collin de l'Hortet A, Wang Y, Handa K, Guzman-Lepe J, Matsubara K, et al. Assembly and function of a bioengineered human liver for transplantation generated solely from induced pluripotent stem cells. *Cell Rep*. 2020;31:107711.
- Telias M, Ben-Yosef D. Modeling neurodevelopmental disorders using human pluripotent stem cells. *Stem Cell Rev Rep*. 2014;10:494–511.
- Takahashi K, Tanabe K, Ohnuki M, Narita M, Ichisaka T, Tomoda K, et al. Induction of pluripotent stem cells from adult human fibroblasts by defined factors. *Cell*. 2007;131:861–72.
- Song Z, Cai J, Liu Y, Zhao D, Yong J, Duo S, et al. Efficient generation of hepatocyte-like cells from human induced pluripotent stem cells. *Cell Res*. 2009;19:1233–42.
- Sampaziotis F, Cardoso de Brito M, Madrigal P, Bertero A, Saeb-Parsy K, Soares FAC, et al. Cholangiocytes derived from human induced pluripotent stem cells for disease modeling and drug validation. *Nat Biotechnol*. 2015;33:845–52.
- Ogawa M, Ogawa S, Bear CE, Ahmadi S, Chin S, Li B, et al. Directed differentiation of cholangiocytes from human pluripotent stem cells. *Nat Biotechnol*. 2015;33:853–61.
- De Assuncao TM, Sun Y, Jalan-Sakrikar N, Drinane MC, Huang BQ, Li Y, et al. Development and characterization of human-induced pluripotent stem cell-derived cholangiocytes. *Lab Invest*. 2015;95:684–96.
- Sampaziotis F, de Brito MC, Geti I, Bertero A, Hannan NR, Vallier L. Directed differentiation of human induced pluripotent stem cells into functional cholangiocyte-like cells. *Nat Protoc*. 2017;12:814–27.
- Collin de l'Hortet A, Takeishi K, Guzman-Lepe J, Morita K, Achreja A, Popovic B, et al. Generation of human fatty livers using custom-engineered induced pluripotent stem cells with modifiable SIRT1 metabolism. *Cell Metab*. 2019;30:e389.
- Karagiannis P, Takahashi K, Saito M, Yoshida Y, Okita K, Watanabe A, et al. Induced pluripotent stem cells and their use in human models of disease and development. *Physiol Rev*. 2019;99:79–114.
- Zabulica M, Srinivasan RC, Vosough M, Hammarstedt C, Wu T, Gramignoli R, et al. Guide to the assessment of mature liver gene expression in stem cell-derived hepatocytes. *Stem Cells Dev*. 2019;28:907–19.
- Takebe T, Wells JM. Organoids by design. *Science*. 2019;364:956–9.
- Ouchi R, Togo S, Kimura M, Shinozawa T, Koido M, Koike H, et al. Modeling steatohepatitis in humans with pluripotent stem cell-derived organoids. *Cell Metab*. 2019;30:e376.
- Feranchak AP, Fitz JG, Roman RM. Volume-sensitive purinergic signaling in human hepatocytes. *J Hepatol*. 2000;33:174–82.
- Banales JM, Huebert RC, Karlens T, Strazzabosco M, LaRusso NF, Gores GJ. Cholangiocyte pathobiology. *Nat Rev Gastroenterol Hepatol*. 2019;16:269–81.
- Colombo C, Battezzati PM. Liver involvement in cystic fibrosis: primary organ damage or innocent bystander? *J Hepatol*. 2004;41:1041–4.
- Li Q, Dutta A, Kresge C, Bugde A, Feranchak AP. Bile acids stimulate cholangiocyte fluid secretion by activation of transmembrane member 16A Cl(-) channels. *Hepatology*. 2018;68:187–99.
- Dutta AK, Woo K, Khimji AK, Kresge C, Feranchak AP. Mechanosensitive Cl- secretion in biliary epithelium mediated through TMEM16A. *Am J Physiol Gastrointest Liver Physiol*. 2013;304:G87–98.
- Dutta AK, Khimji A-K, Kresge C, Bugde A, Dougherty M, Esser V, et al. Identification and functional characterization of TMEM16A, a Ca²⁺-activated Cl- channel activated by extracellular nucleotides, in biliary epithelium. *J Biol Chem*. 2011;286:766–76.
- Guo J-W, Liu X, Zhang T-T, Lin X-C, Hong YU, Yu J, et al. Hepatocyte TMEM16A deletion retards NAFLD progression by ameliorating hepatic glucose metabolic disorder. *Adv Sci (Weinh)*. 2020;7:1903657.
- Feranchak AP, Roman RM, Doctor RB, Salter KD, Toker A, Fitz JG. The lipid products of phosphoinositide 3-kinase contribute to regulation of cholangiocyte ATP and chloride transport. *J Biol Chem*. 1999;274:30979–86.
- Voss FK, Ullrich F, Münch J, Lazarow K, Lutter D, Mah N, et al. Identification of LRRC8 heteromers as an essential component

- of the volume-regulated anion channel VRAC. *Science*. 2014;344:634–8.
24. Qiu Z, Dubin A, Mathur J, Tu B, Reddy K, Miraglia L, et al. SWELL1, a plasma membrane protein, is an essential component of volume-regulated anion channel. *Cell*. 2014;157:447–58.
 25. Fiorotto R, Strazzabosco M. Pathophysiology of cystic fibrosis liver disease: a channelopathy leading to alterations in innate immunity and in microbiota. *Cell Mol Gastroenterol Hepatol*. 2019;8:197–207.
 26. Park JH, Ousingsawat J, Cabrita I, Bettels RE, Große-Onnebrink J, Schmalstieg C, et al. TMEM16A deficiency: a potentially fatal neonatal disease resulting from impaired chloride currents. *J Med Genet*. 2021;58:247–53.
 27. Li P, Hu M, Wang CE, Feng X, Zhao ZhuangZhuang, Yang Y, et al. LRRC8 family proteins within lysosomes regulate cellular osmoregulation and enhance cell survival to multiple physiological stresses. *Proc Natl Acad Sci U S A*. 2020;117:29155–65.
 28. Schrem H, Klempnauer J, Borlak J. Liver-enriched transcription factors in liver function and development. Part II: The C/EBPs and D site-binding protein in cell cycle control, carcinogenesis, circadian gene regulation, liver regeneration, apoptosis, and liver-specific gene regulation. *Pharmacol Rev*. 2004;56:291–330.
 29. Gardner-Stephen DA, Mackenzie PI. Liver-enriched transcription factors and their role in regulating UDP glucuronosyltransferase gene expression. *Curr Drug Metab*. 2008;9:439–52.
 30. Trefts E, Gannon M, Wasserman DH. The liver. *Curr Biol*. 2017;27:R1147–51.
 31. Morio B, Panthu B, Bassot A, Rieusset J. Role of mitochondria in liver metabolic health and diseases. *Cell Calcium*. 2021;94:102336.
 32. Strable MS, Ntambi JM. Genetic control of de novo lipogenesis: role in diet-induced obesity. *Crit Rev Biochem Mol Biol*. 2010;45:199–214.
 33. Lemos FO, Florentino RM, Lima Filho ACM, Dos Santos ML, Leite MF. Inositol 1,4,5-trisphosphate receptor in the liver: expression and function. *World J Gastroenterol*. 2019;25:6483–94.
 34. Stutts MJ, Canessa CM, Olsen JC, Hamrick M, Cohn JA, Rossier BC, et al. CFTR as a cAMP-dependent regulator of sodium channels. *Science*. 1995;269:847–50.
 35. Mansini AP, Peixoto E, Thelen KM, Gaspari C, Jin S, Grdilone SA. The cholangiocyte primary cilium in health and disease. *Biochim Biophys Acta Mol Basis Dis*. 2018;1864:1245–53.
 36. Dutta AK, Woo K, Doctor RB, Fitz JG, Feranchak AP. Extracellular nucleotides stimulate Cl⁻ currents in biliary epithelia through receptor-mediated IP₃ and Ca²⁺ release. *Am J Physiol Gastrointest Liver Physiol*. 2008;295:G1004–15.
 37. Scudellari M. How iPSC cells changed the world. *Nature*. 2016;534:310–2.
 38. Musunuru K, Sheikh F, Gupta RM, Houser SR, Maher KO, Milan DJ, et al. Induced pluripotent stem cells for cardiovascular disease modeling and precision medicine: a scientific statement from the American Heart Association. *Circ Genom Precis Med*. 2018;11:e000043.
 39. Giandomenico SL, Sutcliffe M, Lancaster MA. Generation and long-term culture of advanced cerebral organoids for studying later stages of neural development. *Nat Protoc*. 2021;16:579–602.
 40. Corbett JL, Duncan SA. iPSC-derived hepatocytes as a platform for disease modeling and drug discovery. *Front Med (Lausanne)*. 2019;6:265.
 41. Jin M, Yi X, Liao W, Chen QI, Yang W, Li Y, et al. Advancements in stem cell-derived hepatocyte-like cell models for hepatotoxicity testing. *Stem Cell Res Ther*. 2021;12:84.
 42. Akbari S, Sevinç GG, Ersoy N, Basak O, Kaplan K, Sevinç K, et al. Robust, long-term culture of endoderm-derived hepatic organoids for disease modeling. *Stem Cell Reports*. 2019;13:627–41.
 43. Wang Z, Faria J, Penning LC, Masereeuw R, Spee B. Tissue-engineered bile ducts for disease modeling and therapy. *Tissue Eng Part C Methods*. 2021;27:59–76.
 44. Schaub JR, Huppert KA, Kurial SNT, Hsu BY, Cast AE, Donnelly B, et al. De novo formation of the biliary system by TGFβ-mediated hepatocyte transdifferentiation. *Nature*. 2018;557:247–51.
 45. Clotman F, Jacquemin P, Plumb-Rudewicz N, Pierreux CE, Van der Smissen P, Dietz HC, et al. Control of liver cell fate decision by a gradient of TGFβ signaling modulated by Onecut transcription factors. *Genes Dev*. 2005;19:1849–54.
 46. Flynn DM, Nijjar S, Hubscher SG, de Goyet JV, Kelly DA, Strain AJ, et al. The role of Notch receptor expression in bile duct development and disease. *J Pathol*. 2004;204:55–64.
 47. Amirneni S, Haep N, Gad MA, Soto-Gutierrez A, Squires JE, Florentino RM. Molecular overview of progressive familial intrahepatic cholestasis. *World J Gastroenterol*. 2020;26:7470–84.
 48. Riordan JR, Rommens JM, Kerem B-S, Alon N, Rozmahel R, Grzelczak Z, et al. Identification of the cystic fibrosis gene: cloning and characterization of complementary DNA. *Science*. 1989;245:1066–73.
 49. Chen JS, Sabir S, Al Khalili Y. Physiology, Osmoregulation and Excretion. In: StatPearls. Treasure Island, FL: StatPearls Publishing; 2021.

SUPPORTING INFORMATION

Additional supporting information may be found in the online version of the article at the publisher's website.

How to cite this article: Florentino RM, Li Q, Coard MC, Haep N, Motomura T, Diaz-Aragon R, et al. Transmembrane channel activity in human hepatocytes and cholangiocytes derived from induced pluripotent stem cells. *Hepatol Commun*. 2022;6:1561–1573. <https://doi.org/10.1002/hep4.1920>